

# Effects of the magneto-crystalline anisotropy on the magnetic properties of Fe/Cr/Fe (110) trilayer

C.G. Bezerra<sup>1,a</sup>, C. Chesman<sup>1</sup>, E.L. Albuquerque<sup>1</sup>, and A. Azevedo<sup>2</sup>

<sup>1</sup> Departamento de Física, Universidade Federal do Rio Grande do Norte 59072-970, Natal-RN, Brazil

<sup>2</sup> Departamento de Física, Universidade Federal de Pernambuco 50670-901, Recife-PE, Brazil

Received 12 April 2004

Published online 23 July 2004 – © EDP Sciences, Società Italiana di Fisica, Springer-Verlag 2004

**Abstract.** In this paper we present a theoretical study about the influence of the magneto-crystalline anisotropy on the magnetic properties of magnetic metallic trilayers Fe/Cr/Fe (110). The theory is based on a realistic phenomenological model which includes the following contributions to the free magnetic energy: Zeeman, cubic and uniaxial anisotropy, as well as bilinear and biquadratic exchange energies. The experimental parameters used here are based on experimental data known from the literature. We present numerical results of magnetization versus external applied field to illustrate the behavior of the system. Our numerical results show that in some situations the saturation field can not be correctly determined by magnetoresistance measures.

**PACS.** 75.70.Cn Magnetic properties of interfaces (multilayers, superlattices, heterostructures) – 75.30.Gw Magnetic anisotropy – 71.70.Gm Exchange interactions – 75.75.+a Magnetic properties of nanostructures

## 1 Introduction

Since the last decade, the study of magnetic multilayers has been a field of intense activity in physics, from both the theoretical and experimental point of view. In particular, the properties of magnetic interactions between ferromagnetic films separated by nonmagnetic spacers have been widely investigated (for reviews see [1,2], and the references there in).

The magnetic state of a ferromagnet can affect the electrical transport properties of the material in several ways. For example, the relative orientation of the magnetic moments in magnetic multilayers underlies the phenomenon of giant magnetoresistance (GMR) [3]. The inverse effect, in which a large electrical current density can perturb the magnetic state of a multilayer has been predicted [4] and observed experimentally with lithographically patterned samples [5]. Some of these observations were taken as indirect evidence for current-induced excitation of spin waves, and indeed, recently the high-frequency behavior and partial phase coherence of such current-induced excitations was probed, by externally irradiating a point contact with microwaves, supporting the feasibility of a kind of spin-wave maser [6]. Besides, the possibility of applying the giant magnetoresistance effect in information

storage technology [7] as well as in mixed magnetic multilayers used for tailoring new shapes of GMR curves [8], makes this subject an attractive object of applied research.

Magnetic multilayers which incorporate ultrathin ferromagnetic films, are physical realizations of classical, one dimensional spin systems, with spins coupled via exchange mediated by spacer layers subject to anisotropy. Such systems can undergo a rich range of phase transitions, in response to an external magnetic field, or changes in temperature. Since interfilm exchange is weak, modest magnetic fields can induce spin reorientation phase transitions. We thus have a new and diverse class of magnetic materials, with phase diagrams subject to design (see [9] for a review). Very recently, the interface magneto-crystalline anisotropy energy (MAE) in Fe/CeH<sub>2</sub> multilayers had been site and element-specifically isolated by combining soft X-ray resonant magnetic scattering with soft X-ray standing waves. Using the different temperature evolutions of both materials it was demonstrated that the transition metal interface MAE dominates the spin reorientation, while the rare-earth contribution becomes significant only at much lower temperatures [10].

As regards the magnetic interactions, the existence of high-order exchange coupling has been a subject of interest for a long time. Exchange anisotropy occurs at the interface between an antiferromagnetic layer and a ferromagnetic layer, and results in a ferromagnet

<sup>a</sup> e-mail: cbezerra@dfte.ufrn.br

hysteresis loop displaced along the field axis. The temperature dependence of interlayer exchange coupling can be studied theoretically within an *ab initio* approach based on a Green function technique [11]. Domain disorder in exchange-biased magnetic multilayers was recently investigated using off-specular neutron reflectometry [12]

The interest in magnetic metallic multilayers can be justified by the discovery of a number of new physical properties in these systems, such as the antiferromagnetic bilinear coupling [13], the oscillatory behavior of the bilinear coupling [14] and the biquadratic coupling [15], among others. The understanding of these new properties became an exciting challenge from the point of view of basic research. Interactions such as biquadratic coupling, three-site four-spin interaction and four-site four-spin interaction have been discussed by many investigators. In particular, the practical interest in biquadratic interaction started when it had to be added to the usual bilinear Heisenberg exchange to explain some magnetic properties of materials, such as MnAs, TbSb, MnO,  $\alpha$ -MnS, EuSe, rare-earth vanadates, arsenates, and phosphates [16]. Furthermore, it was shown that in some materials a biquadratic-like interaction is dominant (see e.g. [16]). More recently, a strong biquadratic coupling has been found in magnetic metallic multilayers [17] and it is responsible for very interesting effects on the properties of the magnetoresistance and magnetization curves [18]. Some theoretical explanations have been proposed for the origin of the biquadratic term (see e.g. [19]). In particular, for the magnetic metallic multilayers, the origin of the biquadratic term was discussed by Edwards et al. [20] and Slonczewski [21] in the theory associated with higher harmonics in the oscillatory exchange coupling.

As regards the crystallographic orientations, with the advances in experimental growth techniques multilayers of impressive quality and different crystallographic growth directions are now easily synthesized, for instance by means of “sputtering” and Molecular Beam Epitaxy (MBE). In fact, it is now possible to “tailor” magnetic multilayers whose macroscopic properties are subject to design and control by varying the thickness and composition of the layers. Thus, magnetic metallic multilayers presenting very specific properties can be experimentally realized. However, despite the above cited advances, the most part of the research performed about magnetic metallic multilayers has been focused on (100) structures. Therefore, there is a lack of studies considering magnetic metallic multilayers grown in different crystallographic orientations, for example the (110) direction.

The purpose of this article is to investigate the influence of the uniaxial and cubic anisotropy, due to the (110) growth direction, on the magnetic properties of magnetic metallic multilayers. In particular, we are interested in Fe/Cr/Fe (110) trilayers presenting both bilinear and biquadratic exchange couplings. The paper is organized as follows. In Section 2 we present the physical model for a single film, including the crystallographic orientation considered here, and we make comparisons with previous experimental results. Later, we extend the free magnetic en-

ergy (including Zeeman, anisotropy and exchange terms) for the trilayer system. Section 3 is devoted to the discussion of the effects of the biquadratic exchange coupling, relative to the bilinear one, and the magneto-crystalline anisotropy on the magnetization curves. Finally, our findings are summarized in Section 4.

## 2 General theory

### 2.1 Single film

The geometry and the coordinate system employed here and its relation to the crystalline axis are shown in Figure 1. At first, we consider just a magnetic single-crystal film with thickness  $d$  having cubic lattice structure. The coordinate system is chosen so that the  $x'y'$  plane is parallel to the film surface, with the  $x'$  and  $y'$  axes along  $[\bar{1}10]$  and  $[001]$  crystal directions, respectively. We study the situation where the external static magnetic field  $\vec{H}$  is applied in the plane of the film at an arbitrary angle  $\theta_H$  with respect to the  $[\bar{1}10]$  direction. In this case, the equilibrium direction of the magnetization  $\vec{M}$  is also in the  $x'y'$  plane, characterized by the angle  $\theta$ . As is well known, the static properties result from the competition of several magnetic terms which compose the total magnetic free energy of the system. In general, each term tries to align the magnetization of the film along different directions. Therefore, our initial goal is to determine the equilibrium values of  $\theta$  as a function of the external magnetic field  $\vec{H}$  (for each particular value of  $\theta_H$ ). The equilibrium direction of  $\vec{M}$  is determined by the minima of the total magnetic free energy. We consider, for a single film, a magnetic free energy per unit area with three basic contributions, i.e.,

$$E_T = E_z + E_{ca} + E_{ua}. \quad (1)$$

Here  $E_z$  is the Zeeman energy (between the ferromagnetic film and the external applied field), and  $E_{ca}$  and  $E_{ua}$  are the cubic and uniaxial crystalline anisotropy energies (which we assume present in the ferromagnetic film). We should remark that the presence of the uniaxial anisotropy in the free magnetic energy is justified because it has been observed in mono-crystal films (110) [22].

The explicit form of the free magnetic energy per unit area can be written as,

$$E_T = -d\vec{M} \cdot \vec{H} + \frac{dK_{ca}}{|\vec{M}|^4} \left( M_X^2 M_Y^2 + M_X^2 M_Z^2 + M_Y^2 M_Z^2 \right) - \frac{dK_{ua}}{|\vec{M}|^2} (\vec{M} \cdot \vec{\theta}_u)^2. \quad (2)$$

In the above equation,  $\vec{H}$  is the external magnetic field which is applied in the film plane,  $d$  is the thickness of the Fe film,  $\vec{M}$  is the magnetization of the Fe film,  $K_{ca}$  is the cubic anisotropy constant and  $K_{ua}$  is the uniaxial anisotropy constant.

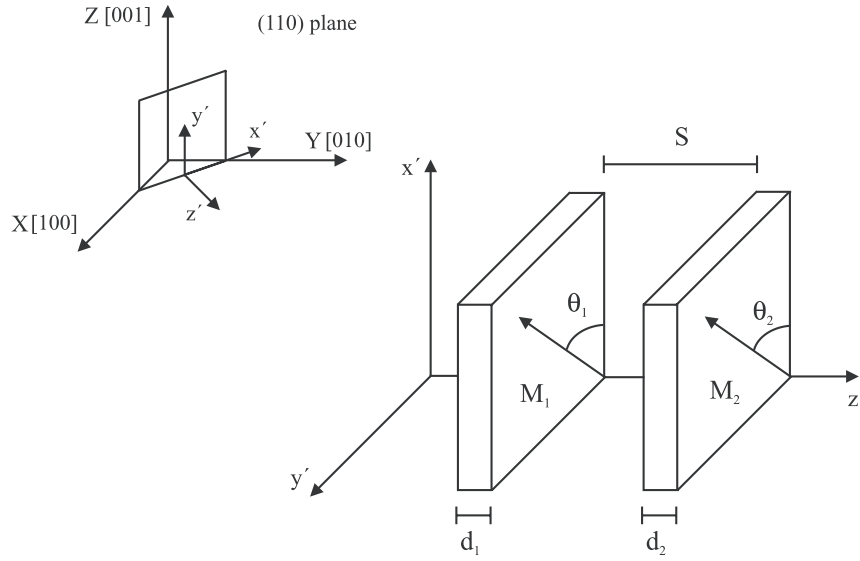


**Fig. 1.** Schematic representation of the trilayer structure and coordinate system considered in this work.

Equation (2), after some calculation, takes the form

$$E_T = -dMH \cos(\theta - \theta_H) + (1/4)dK_{ca} [\cos^4(\theta) + \sin^2(2\theta)] - dK_{ua} \cos^2(\theta - \theta_u), \quad (3)$$

where  $\theta$  is the angular orientation of the magnetization of the Fe film,  $\theta_u$  is the uniaxial anisotropy direction and  $\theta_H$  is the angular orientation of the magnetic field. In order to use the experimental information of reference [22] from this point onwards we consider  $\theta_u = 90^\circ$ , which means that the uniaxial anisotropy renders the [001] direction an easy direction. It is interesting to note that the combination of  $K_{ca}$  and  $K_{ua}$  furnishes a symmetry to the system so that there are an easy axis ( $\theta = 90^\circ$ ), an intermediate axis ( $\theta = 0^\circ$ ) and a hard axis ( $\theta = 35^\circ$ ).

It is usual to write the total free magnetic energy in terms of experimental parameters, or effective fields, for each magnetic term such as,

$$H_{ca} = 2K_{ca}/M_S \quad (4)$$

and

$$H_{ua} = 2K_{ua}/M_S, \quad (5)$$

with  $M_S$  being the saturation magnetization. In this way, we can obtain a final expression for the free magnetic energy per unit area as

$$(E_T/dM_S) = -H \cos(\theta - \theta_H) + (1/8)H_{ca} [\cos^4(\theta) + \sin^2(2\theta)] - (1/2)H_{ua} \cos^2(\theta - \theta_u). \quad (6)$$

Once the values of  $\theta$  that minimize the free magnetic energy are found, we obtain the normalized magnetization

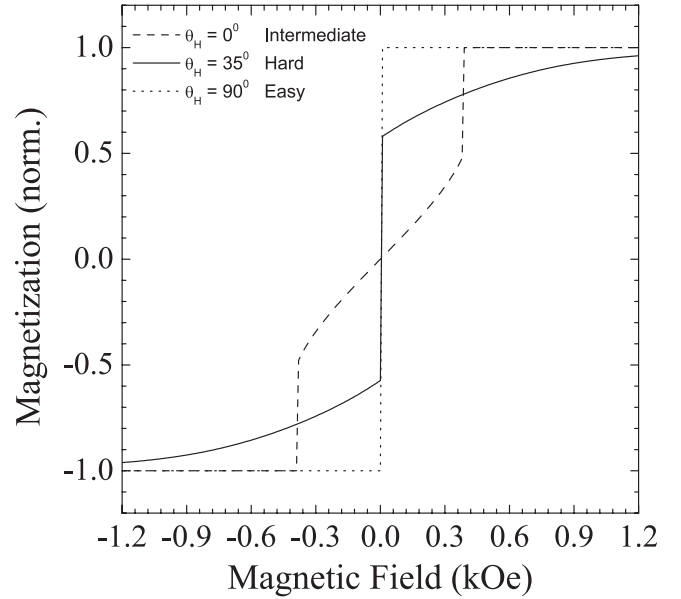


**Fig. 2.** Magnetization curves for a single film with  $\theta_H = 0^\circ$ ,  $35^\circ$  and  $90^\circ$ .

component in the field direction from

$$\frac{M(H)}{M_S} = \frac{M \cos(\theta - \theta_H)}{M_1}. \quad (7)$$

In Figure 2 we have plotted the magnetization versus the external magnetic field for a single film, considering three values of  $\theta_H$ , namely  $\theta_H = 0^\circ$ ,  $35^\circ$  and  $90^\circ$ . These orientations correspond to an intermediate axis, a hard axis and an easy axis, respectively. In our numerical calculations we consider  $H_{ac} = H_{ua} = 0.48$  kOe. These are experimental values which can be found from the literature (see for example [22]). When the field is applied at  $\theta_H = 0^\circ$

there are two phases: the canted phase and the aligned one. For zero field, the magnetization is along the [001] direction and, as the field increases, it rotates towards the field direction until the critical field  $H \sim 0.38$  kOe is reached, for which a first order phase transition occurs and the aligned phase emerges. For  $\theta_H = 35^\circ$  the canted and aligned phases are again present. However, the system goes from the canted phase to the aligned one through a second order phase transition, i.e., as the field is increased the magnetization of the film continuously rotates towards the field direction. The saturation field is around  $H \sim 1.2$  kOe. Finally, when the field is applied at  $\theta_H = 90^\circ$ , which corresponds to an easy axis, only the aligned phase is present. We should remark that our theoretical result, depicted in Figure 2, is in excellent agreement with the experimental result of Prinz et al. [22] (its Fig. 8) who have grown Fe films on GaAs substrate for the first time by means of MBE.

## 2.2 Trilayer system

For the trilayer system the geometry is very similar to the single film case one (see Fig. 1). We consider two magnetic single-crystal films, 1 and 2, having cubic lattice structure. They have thicknesses  $d_1 = d_2 = d$  and are separated by a nonmagnetic spacer layer with thickness  $s$ . As before, we study the situation where the external static magnetic field  $\vec{H}$  is applied in the plane of the films, at an arbitrary angle  $\theta_H$  with respect to the  $[\bar{1}10]$  direction. Therefore, the equilibrium directions of the magnetization of the two films,  $\vec{M}_1$  and  $\vec{M}_2$ , are also in the  $x'y'$  plane, characterized by the angles  $\theta_1$  and  $\theta_2$ . Thus, we have to determine the equilibrium values of  $\theta_1$  and  $\theta_2$  as a function of the external applied field  $\vec{H}$ . In a similar way to the single film case, the equilibrium directions of  $\vec{M}_1$  and  $\vec{M}_2$  are determined by the minima of the total magnetic free energy. However, the magnetic free energy per unit area is composed now by five contributions, the three previous contributions listed in equation (1) plus the exchange energies associated to the bilinear and biquadratic exchange couplings, i.e.,

$$E_T = E_z + E_{ca} + E_{ua} + E_{bl} + E_{bq}. \quad (8)$$

Here  $E_{bl}$  and  $E_{bq}$  are the bilinear and the biquadratic exchange coupling energies (between the ferromagnetic films), respectively.

The form of the free magnetic energy is easily extended for two coupled films yielding

$$E_T = - \sum_{i=1}^{n=2} d_i \vec{M}_i \cdot \vec{H} + \sum_{i=1}^{n=2} \frac{d_i K_{ca}}{|\vec{M}_i|^4} \left( M_{iX}^2 M_{iY}^2 + M_{iX}^2 M_{iZ}^2 + M_{iY}^2 M_{iZ}^2 \right) - \sum_{i=1}^{n=2} \frac{d_i K_{ua}}{|\vec{M}_i|^2} (\vec{M}_i \cdot \vec{\theta}_u)^2 - J_{bl} \frac{\vec{M}_1 \cdot \vec{M}_2}{|\vec{M}_1| |\vec{M}_2|} + J_{bq} \frac{(\vec{M}_1 \cdot \vec{M}_2)^2}{|\vec{M}_1|^2 |\vec{M}_2|^2}, \quad (9)$$

which can be written as

$$E_T/dM_S = - \sum_{i=1}^{n=2} H \cos(\theta_i - \theta_H) + \sum_{i=1}^{n=2} (1/8) H_{ca} \left[ \cos^4(\theta_i) + \sin^2(2\theta_i) \right] - \sum_{i=1}^{n=2} (1/2) H_{ua} \cos^2(\theta_i - \theta_u) - H_{bl} \cos(\theta_1 - \theta_2) + H_{bq} \cos^2(\theta_1 - \theta_2). \quad (10)$$

Here we have used

$$H_{bl} = J_{bl}/dM_S, \quad (11)$$

as the bilinear exchange coupling field, which favors anti-ferromagnetic alignment when negative and ferromagnetic alignment when positive, and

$$H_{bq} = J_{bq}/dM_S, \quad (12)$$

as the biquadratic exchange coupling field, which is experimentally found to be positive and favors a non-collinear alignment ( $90^\circ$ ) between two adjacent magnetizations.

## 3 Numerical results

In this section we present the numerical results obtained for the magnetization curves of the trilayer system. In all situations, as before, we have considered the cubic anisotropy effective field equal to the uniaxial anisotropy one, i.e.,  $H_{ca} = H_{ua} = 0.48$  kOe, as well as  $\theta_u = 90^\circ$ . In our calculations we have used three sets of experimental values for the bilinear and biquadratic exchange couplings, namely:

- (i) the first one with  $H_{bl} = -1.0$  kOe and  $H_{bq} = 0.1$  kOe;
- (ii) the second one with  $H_{bl} = -0.15$  kOe and  $H_{bq} = 0.05$  kOe;
- (iii) the third one with  $H_{bl} = -0.05$  kOe and  $H_{bq} = 0.05$  kOe.

These experimental sets are known from the literature [17] and they are suitable for comparisons with previous works [18]. For each experimental set of the exchange energies, the external magnetic field is applied in three specific orientations:  $\theta_H = 0^\circ$ ,  $\theta_H = 35^\circ$  and  $\theta_H = 90^\circ$ . Once the equilibrium orientations of the each individual film,  $\theta_1$  and  $\theta_2$ , are found, we obtain normalized values for the normalized magnetization component in the field direction from

$$\frac{M(H)}{M_S} = \frac{M_1 \cos(\theta_1 - \theta_H) + M_2 \cos(\theta_2 - \theta_H)}{M_1 + M_2}. \quad (13)$$

In Figure 3 we show the curves of the normalized magnetization versus magnetic field for the first set of exchange couplings. When  $\theta_H = 0$ , at the low field region, the magnetizations are antiparallel, due to the strong bilinear field, and lie on the easy axis (at  $90^\circ$  from the  $[\bar{1}10]$  direction). As the field is increased, the magnetizations symmetrically rotate toward the field direction, and the

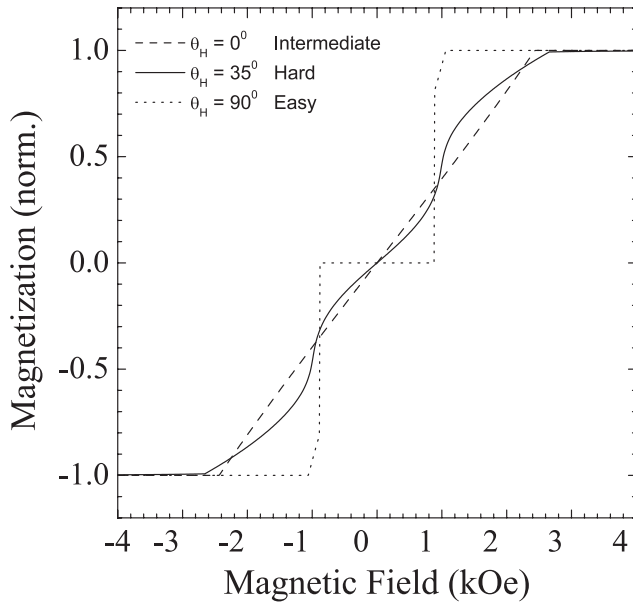


**Fig. 3.** Magnetization curves for a trilayer system, for the first set of exchange fields, with  $\theta_H = 0^\circ$ ,  $35^\circ$  and  $90^\circ$ .

saturation is reached at  $H \sim 2.44$  kOe. For  $\theta_H = 35^\circ$ , the magnetizations are only nearly antiparallel at the low field region. However, they rotate asymmetrically as the field is increased. This asymmetric phase prevails until  $H \sim 0.96$  kOe, for which a second order phase transition occurs and a  $90^\circ$  phase emerges. The saturation is reached at  $H \sim 2.65$  kOe. When the field is applied at  $\theta_H = 90^\circ$ , as expected, the magnetizations remain antiparallel until a first order phase transition occurs at  $H \sim 0.89$  kOe. A symmetric phase emerges and prevails until the saturation is reached at  $H \sim 1.06$  kOe. There are no major differences between the behavior of (100)- and (110)-trilayers for this set of exchange energies (see [18]).

Magnetizations curves found for the second set of exchange fields are shown in Figure 4. For  $\theta_H = 0^\circ$ , the magnetizations are only nearly antiparallel even at the low field region. This is because the biquadratic field is now  $\sim 33\%$  of the bilinear one. As the field is increased, the magnetizations symmetrically rotate continuously toward the field direction until the saturation is reached at  $H \sim 0.78$  kOe. When  $\theta_H = 35^\circ$  an interesting configuration occurs. The magnetizations rotate asymmetrically toward the field direction until  $H \sim 0.27$  kOe is reached, for which there is a first order phase transition and both magnetizations *stay aligned before saturation* at  $\theta_1 = \theta_2 \sim 80^\circ$ , from the  $[\bar{1}10]$  direction. As the field increases, they rotate together until the saturation is reached at  $H \sim 2.1$  kOe. Finally, for  $\theta_H = 90^\circ$ , the antiparallel phase prevails in the low field region until  $H \sim 0.15$  kOe, where a first order phase transition to the aligned phase occurs.

Figure 5 shows the numerical results of the magnetization curves for the third set of the exchange fields which means  $|H_{bl}| = H_{bq}$ . For  $\theta_H = 0^\circ$ , as in the previous set, the magnetizations are only nearly antiparallel at the low field region, due to the strong relative intensity of biquadratic

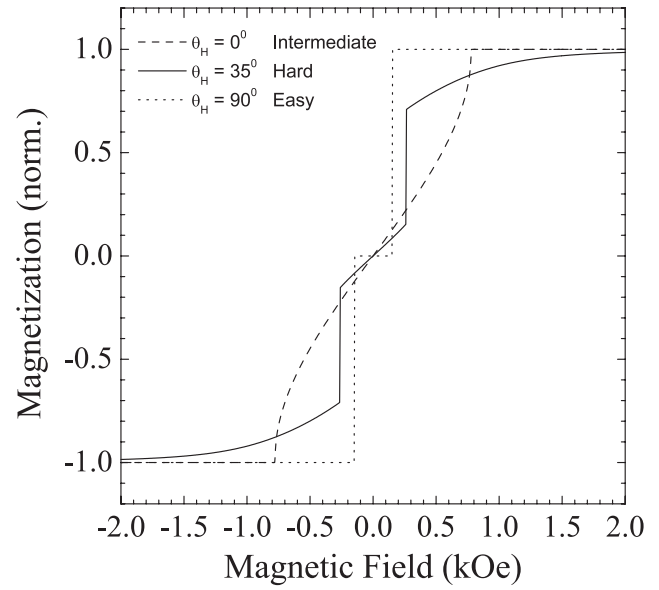


**Fig. 4.** Same as in Figure 3 but for the second set of exchange fields.

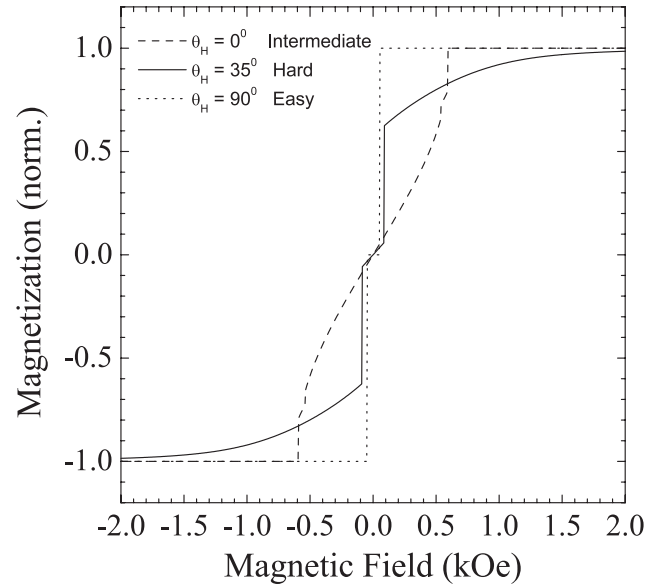


**Fig. 5.** Same as Figure 3, but for the third set of exchange fields.

field (which is now 100% of the bilinear one). The magnetizations rotate symmetrically toward the field direction until  $H \sim 0.54$  kOe, for which a first order phase transition occurs to an asymmetric phase. The saturation is reached at  $H \sim 0.6$  kOe. For  $\theta_H = 35^\circ$ , as in the previous set of exchange fields, the magnetizations rotate continuously toward the field direction until  $H \sim 0.09$  kOe, where a first order phase transition occurs to a phase for which again the magnetizations *stay aligned before saturation* at  $\theta_1 = \theta_2 \sim 85^\circ$ , from the  $[\bar{1}10]$  direction, and rotate together until the saturation is reached at  $H \sim 2.5$  kOe. Finally, for  $\theta_H = 90^\circ$ , the antiferromagnetic phase prevails

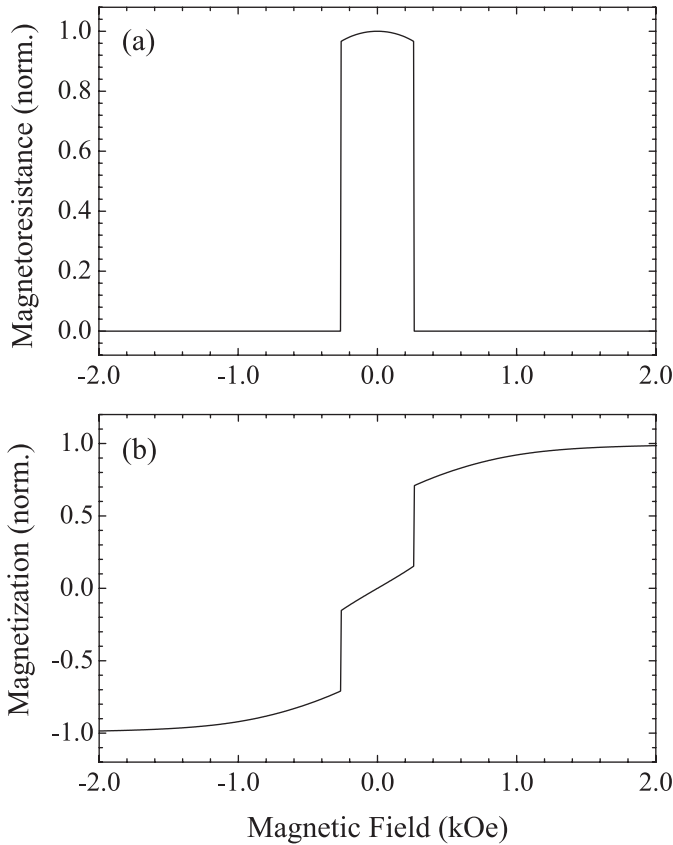


**Fig. 6.** (a) Magnetoresistance and (b) Magnetization curves for the second set of exchange energies.

until  $H \sim 0.06$  kOe, when a first order phase transition occurs to the aligned phase.

Let us take a closer look at the consequences of the configuration obtained for  $\theta_H = 35^\circ$  in the two previous sets of exchange energies. It has been shown that magnetoresistance varies linearly with  $\cos(\Delta\theta)$  when electrons form a free-electron gas, i.e., there are no barriers between adjacent films [23]. Here,  $\Delta\theta$  is the angular difference between adjacent magnetizations. In metallic systems such as Fe/Cr this angular dependence is valid. It is known from the literature that in (100) Fe/Cr/Fe trilayers, magnetoresistance and magnetization curves furnish the same saturation field [17, 18]. However, according to our results for the second and third sets of exchange couplings for (110) Fe/Cr/Fe (with external field applied at  $\theta_H = 35^\circ$ ), magnetoresistance and magnetization curves furnish different values for the saturation field. This is because the magnetizations get parallel before align to the magnetic applied field, due to the (110) magneto-crystalline anisotropy. This is well illustrated in Figure 6 for the second set of exchange energies (a similar behavior is found for the third set). It is very clear from the figure that the magnetoresistance reaches saturation before magnetization. However, for the best of our knowledge, there is so far no experimental evidence to support this amazing theoretical achievement.

## 4 Conclusions

In summary, we have studied the effects of the magneto-crystalline anisotropy on the magnetic properties of magnetic metallic trilayers Fe/Cr/Fe (110) presenting bilinear and biquadratic exchanges. We consider the magnetic components of the trilayer system as two magnetic single-crystal films, having cubic lattice structure, separated by a non-magnetic spacer. The calculation is based on a phenomenological model which includes the following contributions to the free magnetic energy: Zeeman, cubic and uniaxial anisotropies, bilinear and biquadratic exchange energies. We have numerically calculated the magnetization curves, assuming three experimental sets of values for the exchange energies, for three different orientations of the external applied field:  $\theta_H = 0^\circ$ ,  $\theta_H = 35^\circ$  and  $\theta_H = 90^\circ$ , corresponding to an intermediate axis, a hard axis and an easy axis, respectively.

Our results for a single film show that the model employed here is a quite realistic one, reproducing very well experimental results known from the literature [22]. Therefore, it is reasonable to extend it to the trilayer system. The magnetization curves for the trilayers Fe/Cr/Fe (110) exhibit a rich variety of configurations induced by the external magnetic field. In particular, we point out an interesting configuration that occurs for  $\theta_H = 35^\circ$ . In this configuration, which is present for the second and third set of exchange fields, both magnetizations *stay aligned before saturation*, i.e.  $\theta_1 = \theta_2$  ( $\sim 80^\circ$  in Fig. 4 and  $\sim 85^\circ$  in Fig. 5), from the  $[\bar{1}10]$  direction. This is because it costs less energy for the magnetizations stay aligned in a different direction than in the field direction, once  $\theta_H = 35^\circ$  corresponds to the hard axis and the exchange fields are weak enough. Such configuration it is not found in trilayers Fe/Cr/Fe (100) [18], even for weak exchange fields, being therefore a *consequence* of the (110) orientation. We also have shown that this configuration leads to different values of the saturation field for magnetization and magnetoresistance curves.

The most appropriate experimental techniques to verify our numerical results are the magneto-optical Kerr effect (MOKE) and magnetoresistance, and we hope that they may stimulate further experimental studies on these structures.

The authors would like to thank the Brazilian Agencies CNPq, MCT-NanoSemiMat and FINEP/CT-Infra, for partial financial support.

## References

1. M.D. Stiles, J. Magn. Magn. Mater. **200**, 332 (1999)
2. B. Heinrich, Can. J. Phys. **78**, 161 (2000)
3. M.N. Baibich, J.M. Broto, A. Fert, F. Nguyen Van Dau, F. Petroff, P. Etienne, G. Creuzet, A. Friederich, J. Chazelas, Phys. Rev. Lett. **61**, 2472 (1988)

4. L. Berger, Phys. Rev. B **54**, 9353 (1996); L. Berger, J. Appl. Phys. **81**, 4880 (1997)
5. E.B. Myers, D.C. Ralph, J.A. Katine, R.N. Louie, R.A. Buhrman, Science **285**, 867 (1999)
6. M. Tsoi, A.G.M. Jansen, J. Bass, W.C. Chiang, V. Tsoi, P. Wyder, Nature **406**, 46 (2000)
7. W.J. Gallagher, S.S.P. Parkin, Y. Lu, X.P. Bian, A. Marley, K.P. Roche, R.A. Altman, S.A. Rishton, C. Jahnes, T.M. Shaw, G. Xiao, J. Appl. Phys. **81**, 3741 (1997)
8. W. Schepper, A. Hutten, G. Reiss, J. Appl. Phys. **88**, 993 (2000)
9. *Ultrathin Magnetic Structures*, edited by B. Heinrich, J.A.C. Bland (Springer-Verlag, Berlin-Heidelberg, 1994)
10. S.S. Dhesi, H.A. Durr, M. Munzenberg, W. Felsch, Phys. Rev. Lett. **90**, 117204 (2003)
11. V. Drchal, J. Kudrnovsky, P. Bruno, I. Turek, P.H. Dederichs, P. Weinberger, Phys. Rev. B **60**, 9588 (1999)
12. C.H. Marrows, S. Langridge, M. Ali, A.T. Hindmarch, D.T. Dekadjevi, S. Foster, B.J. Hickey, Phys. Rev. B **66**, 024437 (2002)
13. P. Grünberg, R. Schreiber, Y. Pang, M.O. Brodsky, H. Sowers, Phys. Rev. Lett. **57**, 2442 (1986)
14. S.S.P. Parkin, N. More, K.P. Roche, Phys. Rev. Lett. **64**, 2304 (1990)
15. M. Ruhrig, R. Schafer, A. Hubert, R. Mosler, J.A. Wolf, S. Demokritov, P. Grünberg, Physica Status Solidi (a) **125**, 635 (1991)
16. M. Pavkov, S. Stojanović, D. Kapor, M. Škrinjar, D. Nikolić, Phys. Rev. B **60**, 6574 (1999)
17. A. Azevedo, C. Chesman, S.M. Rezende, F.M. de Aguiar, X. Bian, S.S.P. Parkin, Phys. Rev. Lett. **76**, 4837 (1996); C. Chesman, M.A. Lucena, M.C. de Moura, A. Azevedo, F.M. de Aguiar, S.M. Rezende, S.S.P. Parkin, Phys. Rev. B **58**, 101 (1998)
18. C.G. Bezerra, J.M. de Araújo, C. Chesman, E.L. Albuquerque, Phys. Rev. B **60**, 9264 (1999); C.G. Bezerra, J.M. de Araújo, C. Chesman, E.L. Albuquerque, J. Appl. Phys. **89**, 2286 (2001)
19. P.W. Anderson, Phys. Rev. **115**, 2 (1959); C. Kittel, Phys. Rev. **120**, 335 (1960); N.L. Huang, R. Orbach, Phys. Rev. Lett. **12**, 275 (1964)
20. D.M. Edwards, J.M. Ward, J. Mathon, J. Magn. Magn. Mater. **126**, 380 (1993)
21. J.C. Slonczewski, Phys. Rev. Lett. **67**, 3172 (1991)
22. G.A. Prinz, G.T. Rado, J.J. Krebs, J. Appl. Phys. **53**, 2087 (1982)
23. A. Vedyayev, B. Dieny, N. Ryzhanova, J.B. Genin, C. Cowache, Europhys. Lett. **25**, 465 (1994)